JTTEE5 8:279-295

Peer Reviewed

Thick Laser Coatings: A Review

L. Pawlowski

This article describes the applications of lasers in coating deposition processes. After an introduction concerning the types and principal characteristics of the laser and the emitted light beams, a description of the mechanism of interaction between a laser beam with typical coating materials is presented. The typical laser treatment processes are depicted, and their characteristics are shown. Recent papers on coatings produced in one-step and two-step laser deposition are reviewed. Finally, the emerging applications of laser processes in thermal spray coatings are discussed.

(Submitted 26 November 1998; in revised form 6 April 1999)

Keywords anilox rolls, laser coatings, laser engraving, laser glazing, laser remelting, laser shock treatment, laser solid interaction, laser treatment, rapid prototyping

1. Introduction

Lasers are sophisticated diagnostic and technological tools that have found increasing application in the field of thermal spraying. They are applied in process control to determine the velocity of sprayed particles using laser Doppler velocimetry (LDV) or laser two-focus systems (L2F). Lasers are also applied in quality control of sprayed coatings by many methods of nondestructive techniques (NDT) (Ref 1). Lasers are also used, complementary to thermal spraying, in thin film processes such as chemical vapor deposition (CVD), physical vapor deposition (PVD) (Ref 2), or pulsed laser deposition (PLD) (Ref 3). This article mainly reviews studies on the thick laser coatings produced by one-step and two-step laser depositions.

The one-step laser deposition (1SLD) technique consists of injecting powder into a laser beam where the powder is heated (melted) and subsequently deposited on the substrate, which is simultaneously melted by the laser. The process is similar to deposition techniques by weld surfacing, such as plasma transferred arc (PTA) welding (e.g., Ref 4). The most recent industrial application of 1SLD is rapid prototyping, which enables production of solid pieces having complicated three-dimensional shapes in one process.

Two-step laser deposition (2SLD) consists of a laser treatment of the predeposited coating. The predeposition can be manufactured by many thin and thick coating techniques. Important among the latter processes is thermal spraying, especially with the techniques of atmospheric plasma spraying (APS), vacuum plasma spraying (VPS), or high-velocity oxygen fuel (HVOF) spraying.

The 1SLD and 2SLD processes can be implemented in three different ways (Fig. 1): (a) cladding, in which the coating is chemically different than the substrate; (b) alloying, in which the coating and substrate form an alloy; and (c) hard phase dispersion, in which hard particles form a composite with the substrate.

L. Pawlowski, Laboratory GéPIFRéM (UPRES-EA No. 2698), University of Lille 1, House C5-Second floor, F-59655 Villeneuve d'Ascq Cedex, France. Contact e-mail lech.pawlowski@univ-lille1.fr. (Permanently at University of Artois, Faculty of Applied Sciences, Technoparc Futura, F-62400 Béthune, France; lechpawlowski@compuserve.com).

2. Fundamentals of Laser Technology

The principles of laser design and characteristics are far beyond the scope of the present review. The interested reader can find information in the monograph of Siegman (Ref 5). The present review concerns only the topics related to laser deposition and the treatment of coatings.

The laser radiation is generated in an optical resonator (cavity) that contains an optically active (lasing) medium (gas, CO_2; solid, neodymium-yttrium aluminum garnet (Nd:YAG) or Nd:glass). The medium is initially excited with a gas discharge (CO_2 laser) or a flash of light (Nd:YAG laser), and an electromagnetic wave starts to oscillate in the cavity. The geometry of the cavity determines a wave mode that, in turn, determines a distribution of energy. The energy is radiated as a plane wave from one of its mirrors being partly transparent (Fig. 2).

In most cases, the distribution of energy corresponding to a fundamental mode TEM_{00} is desired. (Mode TEM_{00} is consid-

Nomenclature

APS	atmospheric plasma spraying
CVD	chemical vapor deposition
cw	continuous wave
EBPVD	electron beam physical vapor deposition
HAp	hydroxyapatite
HAZ	heat-affected zone
HVOF	high-velocity oxygen fuel
LDV	laser Doppler velocimetry
LSP	laser shock processing
L2F	laser two-focus system
MMC	metal matrix composites
NDT	nondestructive techniques
PLD	pulsed laser deposition
PVD	physical vapor deposition
PTA	plasma transferred arc
SHS	self-propagating high-temperature synthesis
TBC	thermal barrier coating
TEM	transverse electromagnetical wave
VPS	vacuum plasma spraying
XRD	x-ray diffraction
YAG	yttrium aluminum garnet
1SLD	one-step laser deposition
2SLD	two-step laser deposition

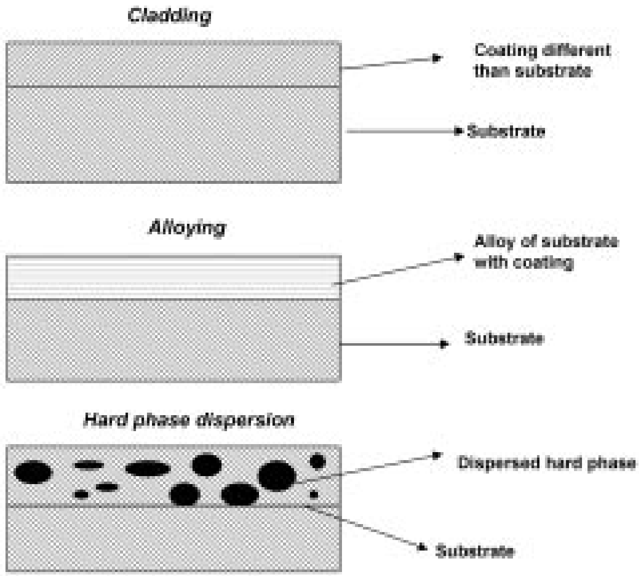

Fig. 1 Schematic representation of the possible variations in one-step and two-step laser deposition techniques

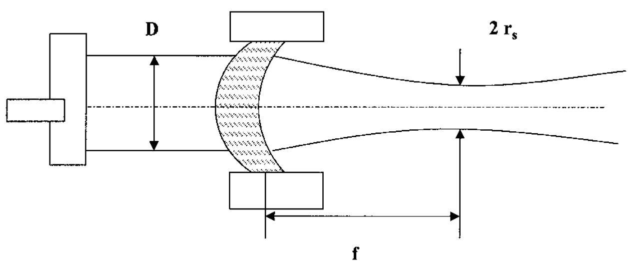

Fig. 3 The focused spot of a laser beam. D, beam diameter; F, focus distance of the lens; r_S, radius of a circle representing the spot area

ered in further discussion.) The quality of laser beam can be described by a factor K. The factor is equal to $K = 1$ for this mode and decreases for higher modes (e.g., $K = 0.57$ for TEM_{01}, Ref 6). However, the modes other than the fundamental one could also be useful sometimes. For example, the TEM_{01} mode was proven to be better than TEM_{00} for the engraving of fine pattern anilox rolls (Ref 7). The light emitted by lasers is monochromatic (one wavelength) and is coherent spatially. The lasers discussed here have a wavelength of 10.6 μm (CO_2 laser) and 1.06 μm (Nd:YAG and Nd:glass lasers). The laser beams are slightly divergent (typically by a degree of a few milliradians). The important property of the laser treatment is the power density. The density, q, is defined for a continuous wave (cw) laser as:

$$q = \frac{P}{S} \qquad \text{(Eq 1)}$$

and for pulsed lasers as:

$$q = \frac{E}{S\tau} \qquad \text{(Eq 2)}$$

where P is a laser power, S is a beam area, E is a pulse energy, and τ is a pulse duration. The power density determines the kind of laser treatment (Table 1).

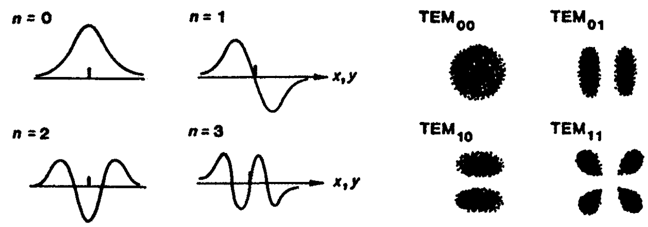

Fig. 2 Transverse modes of the electromagnetic wave inside laser cavity (left side) and corresponding sections of energy distribution of emitted beam (right side)

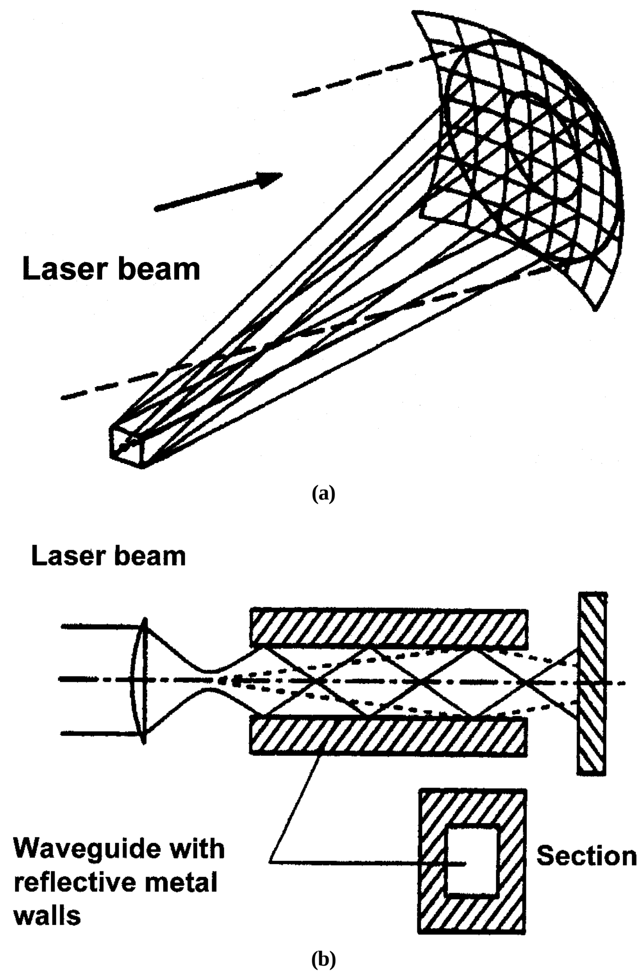

Fig. 4 The examples of integrators used to shape laser beams; (a) segmented mirror and (b) kaleidoscope

For high power density applications (e.g., engraving, LSP) the beam is focused on the substrate (Fig. 3), and the spot area is a circle with a radius r_S. The radius, r_S, depends on the wavelength, beam quality factor, K, and on the properties of the focusing lens in the following fashion (Ref 6):

$$r_S \cong \frac{2\lambda}{\pi}\frac{f}{D}\frac{1}{K} \qquad \text{(Eq 3)}$$

where λ is the wavelength, f is the focus distance of the lens, and D is the beam diameter. It is clear that short wavelength, high

Table 1 Laser power densities used for different treatment types

Treatment No.	Laser treatment type	Power density, kW/cm^2	Phase of treated coating	Treatment applications
1	cw and pulsed	<1	Solid	Phase transformation, heating
2	cw and pulsed	$1\text{-}10^3$	Liquid	Alloying, cladding, hard phase dispersion, rapid prototyping
3	Pulsed, τ = microseconds to milliseconds	$>10^3$	Vapor	Engraving
4	Pulsed, τ = nanoseconds	$>10^6$	Solid	Laser shock processing

cw, continuous wave; τ, pulse duration

beam quality, and a large diameter lens with a short focus distance are necessary to obtain a small spot area.

For low power density applications (heating, 1SLD, 2SLD), the beams should be shaped with the use of integrators (segmented mirror, kaleidoscope, etc.) to obtain the practical rectangular spots (Fig. 4).

The segmented mirror is composed of many polished molybdenum plates that are arranged to superimpose their image in a plane (Ref 8). The kaleidoscope is a waveguide with internal reflective walls (typically polished copper). The beam is reflected many times and emerges well homogenized.

The laser beam is focused on the surface of treated material. For low laser power densities, the fraction of the absorbed density by the treated material, *r*, at the depth, *x*, below the irradiated surface ($x = 0$ at the surface) is given by the following:

$$r = (1 - R)\exp\left(-\frac{x}{L}\right) \quad \text{(Eq 4)}$$

where *R* is a reflectivity and *L* is an optical absorption depth at which the power density decreases by a factor $1/e$ ($e \cong 2.718$). The values of *R* and *L* for some materials are collected in Table 2.

Metals reflect a major part of the laser energy ($R \approx 1$ for far infrared at $\lambda = 10$ µm; see Table 2). The radiation of $\lambda = 1$ µm is less reflected. Thus, the Nd:YAG laser is a better tool to treat metals and alloys than the CO_2 laser. The laser light has a frequency of more than 10^{13} Hz and is absorbed by an energy coupling with free electrons in metals and alloys (Ref 11). Thus, the optical absorption depth is typically smaller than 1 µm for these materials.

Ceramics have a completely filled valence band, and no free electrons are available. The radiation is absorbed by the high-frequency phonons. The energy coupling is weak, and the laser radiation is absorbed much deeper (centimeters or meters below the surface). Quite often, materials such as ceramics are totally transparent (Table 2). The far infrared radiation is better absorbed by ceramics, and the CO_2 laser is a more useful tool to treat this class of materials. (CO_2 laser radiation cannot be conducted by SiO_2 optical fibers. On the other hand, the Nd:YAG laser radiation can be conducted by these fibers. Therefore, the Nd:YAG laser, coupled to fiber, is used for many automatic operations in industry.) A simple technological solution to improve the absorption of laser radiation is the application of a coating of absorbing material (e.g., graphite or black paint) to the surface of the treated sample. The light energy is transformed in thermal energy and increases the temperature at the

Table 2 Optical data for selected metals and oxides at wavelengths of about 1 and 10 µm

Material	Wavelength (λ), µm	Reflectivity (R), dimensionless	L, µm
Al	9.54	0.99	0.21
	0.83	0.87	0.022
Ni	9.54	0.98	0.14
	1.03	0.72	0.046
W	10	0.98	0.16
	1	0.58	0.068
SiO_2	10.6	0.2	40
	1.06	0.04	$>10^6$

L, optical absorption depth at which the power density decreases by a factor $1/e$ ($e = 2.718 \ldots$). Source: Ref 9, 10

surface of the material. The temperature decreases exponentially with the depth, *x*, of the material, as shown in the following equation:

$$T(x,t) = \frac{(1 - R)q\tau}{\rho c_p \sqrt{\pi}} \; \frac{\exp\left[-x^2/(4at)\right]}{\sqrt{4at}} \quad \text{(Eq 5)}$$

where $T(x,t)$ is a temperature distribution (assuming the semi-infinite body approximation) in the materials submitted at the surface ($x = 0$) in a moment of time ($t = 0$) to a laser pulse of power density *q* and a duration, τ. ρ is density, c_p is specific heat, and *a* is thermal diffusivity (Ref 12, 13).

At higher laser power densities, materials start to evaporate, and these vapors absorb a major part of the incoming power. The gas gets ionized, and the plasma can reach high temperatures (Ref 14). The absorption of the radiation by plasma renders laser treatment less efficient while engraving or drilling. On the other hand, the formation of such a plasma enabled a new process called laser shock processing (LSP) or, as in Ref 15, shot peening with laser, to be developed.

Laser shock processing was developed in the 1960s and 1970s (Ref 16). The technique uses the shock waves created by the expansion of a plasma. The plasma results from an interaction of a laser pulse having a power density $q = 1$ to 10 GW/cm^2 and a duration $\tau = 1$ to 30 ns (Ref 17) with the material. To achieve such short pulses, the laser should be equipped with a Q-switch (Ref 5).

Two LSP treatment methods are possible: (a) direct ablation, in which plasma is in direct contact with the coating, and (b) confined treatment, in which the plasma contacts a double layer sys-

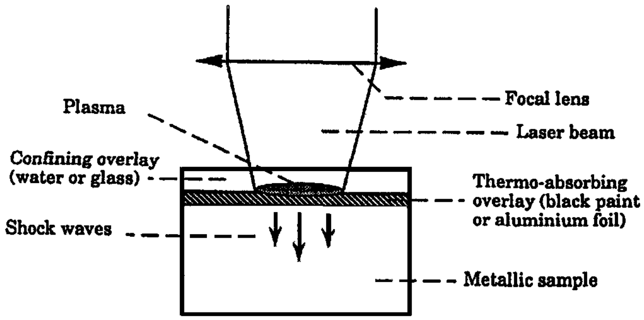

Fig. 5 Confined treatment with laser shocks. Source: Ref 18

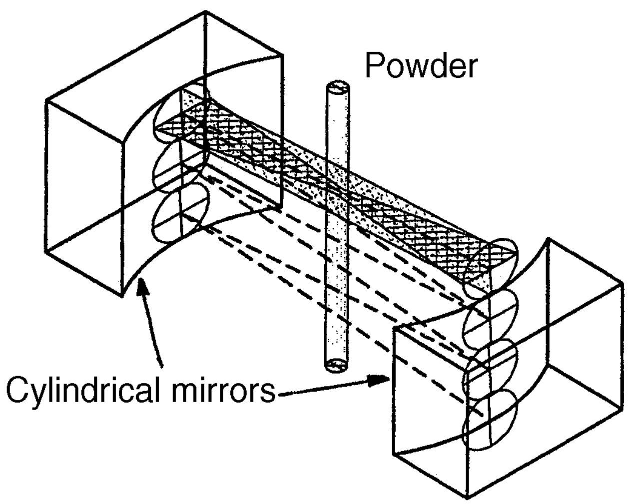

Fig. 7 Sketch of a powder injection into a beam trap. Source: Ref 23

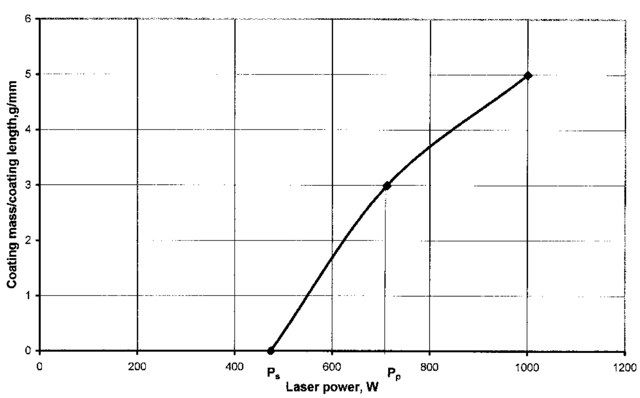

Fig. 9 The deposited mass of coating on a unit length of laser pass versus laser power while cladding Stellite powder onto a stainless steel substrate using a coaxial nozzle (Ref 25). Theoretically calculated points correspond to P_S, melting of substrate, and P_{sp}, melting of substrate and powder

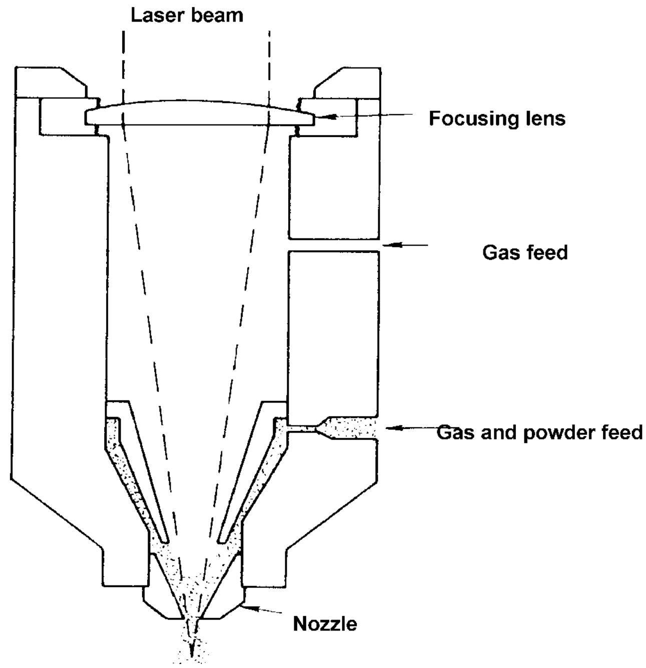

Fig. 6 Sketch of coaxial powder injection. Source: Ref 21, 22

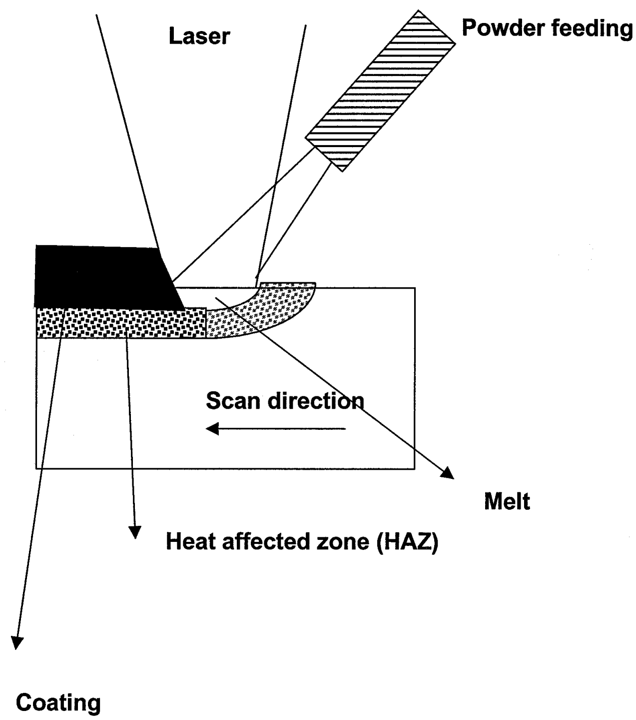

Fig. 8 Powder injection in one-step laser deposition

tem (Fig. 5). The advantage of the latter method is in preventing the coating from contacting a hot plasma (Ref 19) and in increasing (3 to 5 times) the pressure of the shock wave (Ref 20). In the confined treatment, the laser beam crosses the transparent water overlay and is absorbed in a metallic target (aluminum foil). The foil is partly vaporized and creates the expanding plasma. An incoming water flow confines this expansion in a direction opposite to the coating (Ref 18). The pressures of laser shocks measured in the treated substrates with piezoelectric gages are in a range of 3 (Ref 16) to 10 GPa (Ref 20). The pressure, p (in GPa), acting on a treated sample surface, depends on the laser power density, q (in W/cm^2) in the following way (Ref 17):

Table 3 **Characteristics of industrial lasers applied in coating deposition**

Parameter	Laser type	
	CO_2	Nd:YAG
Wavelength, μm	10.6	1.06
Excitation technique	Gas discharge at low pressure	Flash or arc lamp
Pulsed/cw	Both	Both
Maximum average power, kW	25	2
Maximum pulse power, kW	10	100
Beam quality	Very high	Low
Efficiency, %	5-10	2-5
Price(a), 10^3 DM	250, for a laser having an average power of 1 kW	400, for a laser having an average power of 1 kW

(a) Prices in 1991, $1 (U.S.) = 1.63 DM in Oct 1998. Source: Ref 6

$$p = 3.22 \times 10^{-9}\sqrt{q} \quad \text{(Eq 6)}$$

The increase of the laser power density above 10 GW/cm^2 results in a dielectric breakdown in water rather than in a further increase of the shock pressure.

The industrial lasers used to deposit and treat coatings are mainly CO_2 and Nd:glass or Nd:YAG laser. Their properties are collected in Table 3. Another important type of industrial laser, the excimer laser, is used for polymer surface treatment or drilling processes and is not discussed here.

The most important variables of laser treatment processes are collected in Table 4.

Table 4 **Principal process variables in thick coating laser deposition**

Process element	Variable
Laser and optical system	Wavelength
	cw or pulsed (pulse duration)
	Focusing lens (diameter, focus)
	Beam quality
	Beam shape
Treated material	Chemistry
	Initial temperature and heat evacuation conditions
	Dimensions and surface preparation (roughness, black paint, etc.)
	Workpiece velocity
	Laser tracks overlapping
Others	Atmosphere (vacuum, inert gas, etc.)
	Powder properties in 1SLD (chemistry, particle size, etc.)
	Powder feed rate in 1SLD
	Predeposited coating in 2SLD (chemistry, thickness, surface roughness, adhesion, etc.)

3. Laser Coating Processes

3.1 One-Step Laser Deposition

The 1SLD methods include three processes: cladding, alloying, and hard phase dispersion. These processes differ by the dilution. Dilution, expressed in percent, is defined as a ratio of the thickness of a zone where the substrate material is diluted in a coating to the total coating thickness and is expressed in percent of the substrate in a coating. The dilution is small in the cladding process (less than 10%), and it is equal to 100% for alloying and hard phase dispersion processes. In cladding, the continuous rate of powder feed can be delivered to a nozzle (Fig. 6) or inside a beam trap (Fig. 7). The latter is made of two cylindrical mirrors that trap the beam and enable the powder stream to be laser heated along the length of mirrors.

In the alloying and the hard phase dispersion processes, the powder is injected into a melted zone of the substrate (Fig. 8).

Cladding. The physics of the cladding process using coaxial injection of powder was analyzed in Ref 24 to 27. It was found that there is a minimum power necessary to produce the coating (Fig. 9). This power corresponds to the beginning of substrate melting. The velocity of the Stellite 6 alloy particles was determined using laser Doppler velocimetry (LDV), and the values of 1 to 2.5 m/s were measured (Ref 24). The laser power density necessary for in-flight melt of the particle of this alloy was estimated theoretically to be in the range of $q = 5$ to 7 kW/cm^2.

The cladding of the same material was analyzed theoretically in Ref 26 for a powder injection system shown in Fig. 8. The authors found that the powder efficiency can be as high as 69% for a linearly polarized CO_2 laser beam at high angles of incidence (the angle between a normal to a molten pool and a laser beam axis). Finally, Li and Ma (Ref 27) presented an analytical model that enables estimations of the roughness of the clad coating relative to the overlapping of subsequent laser passes. It was determined that roughness decreases in an oscillating way with overlapping. This parameter is the minimum for overlapping of 29, 59, and 71%. The typical parameters used to clad the alloys and cermets are in Table 5.

The resulting microstructure of the deposit is dendritic with fine arm spacing, and the dendrites are elongated in the direction of heat flow (Fig. 10).

The dendritic microstructure is typical for the rapidly solidified alloys and was observed in clads of Stellite (Ref 33), stainless steel (Ref 34), and a cermet composed of NiCrAl alloy with 6 wt% of yttria-stabilized ZrO_2 (Ref 35). The clad coatings are dense and free of pores. The substrate under the coating is heat affected and the depth of the heat-affected zone (HAZ) is typically a few hundred micrometers. In frequently used steel substrates, the HAZ undergoes a phase transformation and becomes martensitic with an increase of hardness. The coatings obtained with cladding are sometimes applied to combat wet corrosion (Ref 34) or high-temperature oxidation (Ref 35) but are mainly applied to resist wear (Ref 30, 36 to 38).

The cladding of ceramic coatings seems to be difficult because of cracks in the deposits and poor adhesion to metallic substrates. The adhesion is reportedly worse (Ref 39) than in

Peer Reviewed

Fig. 10 Optical micrograph of a cross section of an Inconel alloy clad onto a steel substrate. Source: Ref 32

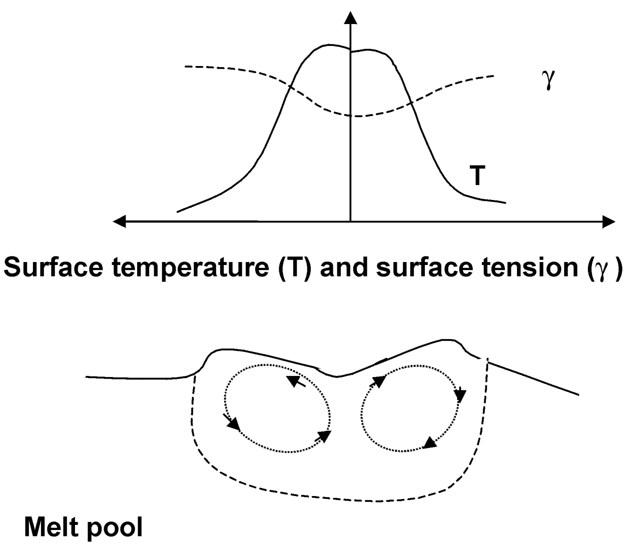

Fig. 11 Surface temperature (T) and surface tension (γ) distribution across a laser melted pool

thermally sprayed ceramics. The use of composites that are rich in ceramic reinforcement, such as self-fluxed nickel-base alloy with 60 vol% of zirconia (Ref 40) or aluminum with chromia reinforcement (Ref 41), can be a solution to obtain ceramiclike clad materials. Such composites could be realized with the use of two separate powder feeders (Ref 42). Laser clad coatings are used for production and repair of rods and rolls in the paper, textile, and food industries, as well as for cutting, punching, or die tools for paper, metal, and glass (Ref 43). At present, cladding seems to be most popular among the 1SLD processes.

Alloying is a process similar to cladding except that another component of the alloy is injected into the molten pool of substrate. Alloying requires a greater laser power density than cladding (Ref 2). The alloying process enables metallic and ceramic alloys, such as nitrides or borides (Ref 2, 44), to be obtained. The process starts with melting of a substrate by laser irradiation. On the surface of a melt pool, there is a temperature distribution, T, which results in the surface tension distribution, γ, shown in Fig. 11. The shear stress, which is equal to the gradient in surface tension, pulls the material from the center and causes convection movement of the melt pool (Ref 45).

In the case of the injection of solid particles into the melt, the convection permits good mixing with the substrate material. The particles are melted, and reaction with the substrate can take place. The reaction slows down and stops soon after the laser beam moves to the next position. The subsequent rapid cooling of the melt makes it possible to form metastable or high-temperature phases as the product of the reaction. However, the cooling rapidity can also be slowed by lowering of laser beam speed over the substrate. The typical parameters of alloying are shown in Table 6.

The laser nitriding of titanium or its alloys has been reported in many papers (Ref 46, 49, 50). Pure TiN was mainly observed near to the surface zone (10 μm thick in Ref 49). The entire coatings were composed of TiN_x and a solid solution of nitrogen in titanium (α Ti or β Ti). Subsequent laser remelting in the nitrogen atmosphere enabled a deeper nitrided zone. One concept in many studies (Ref 47, 48) was to use a laser to form an intermetallic alloy on a metal surface. The alloy was obtained by injection of a powdered second metal into a melted substrate. In this way, aluminum was alloyed with chromium and zinc was alloyed with aluminum (Table 6). Magnesium substrate was alloyed with powders of Al, Cu, Ni, or Si to obtain intermetallic compounds such as $Mg_{17}Al_{12}$, Mg_2Cu, Mg_2Ni, or Mg_2Si (Ref 51), and a mild steel substrate was alloyed with blended powders of Cr, Ni, and Mo to obtain FeCrNiMoC alloy containing austenite with a large amount of martensite phase (Ref 52). The alloyed coatings were studied for use in applications where wear and wet corrosion resistance were required. An application of alloying was reported in the energy generation industry where steam gas turbines blades were coated with titanium nitride (Ref 50). However, the major industrial application of alloying is still to come (Ref 43).

Hard phase dispersion is a coating process that consists of injecting the hard second-phase particles into a melted substrate.

Table 5 Typical parameters used for a laser cladding (CO_2, cw) of alloys and cermets in one-step laser deposition

				Powder			Process parameter				
Alloy	Laser power density (q), kW/cm^2	Mode	Substrate composition, wt%	Composition, wt%	Particle size, μm	Feed rate, g/min	Substrate speed, cm/s	Atmosphere	Injection	Overlapping, %	Ref
Co alloy	4-17	TEM_{01}	Tool steel, 57NiCrMoV77	Co + 28Cr + 5Mo + 3Fe (Stellite 21)	–150+45	6-15	0.17-0.5	…	Coaxial	43-57	28
Ni alloy	4.5	…	…	Ni + 19.5Cr + 13.5Co + 4Mo + 3Ti + 2Fe	–125+44	…	2.5	…	…	25	29
Fe alloy	16-25	…	Low-carbon steel (sand blasted before coating)	Fe + 12Mn + 1.2 C (Hadfield steel)	–100+40	8	0.5-2	Argon	…	42.5	30
Cermet	6-18	TEM_{01}	AISI 1043 stainless steel	WC + 17Co	Average 39	5-20	0.3-1.3	…	Under angle of 60° to normal	…	31

Table 6 Typical parameters used for a laser alloying in one-step laser deposition

				Powder			Process parameter				
Lasing medium	Laser power density (q), kW/cm^2	Mode	Substrate composition, wt%	Composition, wt%	Particle size, μm	Feed rate, g/min	Substrate speed, cm/s	Atmosphere	Overlapping, %	Coating composition	Ref
Titanium substrate with nitrogen gas											
CO_2, cw	9-25	…	Ti + 6Al + 4V	…	…	…	0.3-1.2	N_2/Ar mixture 50/50 and 60/40 per vol continuous flow in a bell jar	15-32	TiN dendritic	46
Aluminum substrate with chromium powder											
	110-260	…	Al + 6Zn + 3Mg + 2Cu (sand blasted before coating)	Blend of Al + 25Cr	–56 (Cr), –150 (Al)	1.8	0.5-4	Ar	50	Al_4Cr, Al_7Cr, Al_{11} Cr	47
Zinc substrate with aluminum powder											
CO_2, cw	Coating, 13; remelting, 31	TEM_{00} + TEM_{01}	99.99Zn	99.99Al	–250	0.6-3.6	0.5	Ar	Coating, 10; remelting, 40	αZn, βAl, eutectic αZn + βAl	48

Table 7 Typical parameters used for a laser hard phase dispersion in one-step laser deposition

				Powder			Process parameter				
Lasing medium	Laser power density (q), kW/cm^2	Mode	Substrate composition, wt%	Composition, wt%	Particle size, μm	Feed rate, g/min	Substrate speed, cm/s	Atmosphere	Injection	Overlapping, %	Ref
Titanium matrix with WC and TiC hard phases											
CO_2, cw	42-140	…	Ti + 6Al + 4V	TiC	–100+50	60-120	5-15	Vacuum, dynamic pressure 40-70 Pa	1 cm from the substrate		53
Aluminum matrix with SiC hard phase											
CO_2, cw	14-89	…	Al + 1Mg + 0.7Si	SiC	–150+105	5-10	0.5-2	Ar, ambient pressure	…	…	56
Titanium matrix with SiC, TiC, TiN hard phase											
Nd:YAG, cw via optic fiber	14-32	…	Ti + 6Al + 4V (sand blasted before coating)	SiC, TiC, TiN	…	1-3	0.8-1.7	Ar, ambient pressure	…	…	55

These particles, contrary to particles in alloying, should remain solid on processing. After solidification, the outer part of the substrate becomes a matrix in which the hard particles are dispersed. This process, which produces metal matrix composites (MMCs), was initiated in the 1970s (Ref 53, 54). Because there is convection in a melting pool, the reinforcement powder injection angle and spot need to be carefully optimized. Kloosterman and De Hosson (Ref 55) found that the powder injection spot should be centered inside a laser beam (position A in Fig. 12). Any other position produces a less homogenous dispersion of particles.

The depth of particle penetration depends on the injection velocity, which is determined, in turn, by the carrier gas flow. An increase in powder feed rate can transform a hard phase dispersion process into a cladding process. Typical processing parameters are collected in Table 7.

The laser power density is comparable to that used in the alloying process. The substrate must melt, but the hard particles are intended to remain solid. To achieve this condition, the temperature of the melt must be well below the melting point of the hard phase. If this is not possible, one can increase the substrate speed to limit the time of particle dissolution in the melt. However, the rapid solidification of the melting pool, which includes particles of hard phase, can generate residual stresses that can lead to cracking of the coating. Cracks can be avoided by preheating the substrate prior to coating (Ref 57). Because the substrates are metals, the application of CO_2 laser is not optimal. For example, the dispersion of SiC in an aluminum matrix by use of such a laser, reported in Ref 56, was not successful. Aluminum absorbs only 1% of the beam energy at this wavelength (see Table 2). Knowing that SiC absorbs CO_2 laser radiation better, the authors placed a layer of silicium carbide on a surface of aluminum. Another solution could have been to use a Nd:YAG laser.

Carbides are used most frequently as a hard phase in the reviewed studies. The coatings obtained often contain the products of their solution in the melt in addition to the initial carbides. Thus, the injection of B_4C in a steel matrix produced Fe_3B and $Fe_{23}B_6$ (Ref 58), and the injection of SiC in an aluminum matrix resulted in $AlSiC_4$ as a solution product (Ref 56). The hard phase dispersion was applied to obtain wear resistant coatings in, for example, polymer extruding machines (Ref 59).

Rapid Prototyping. The total thickness of a coating produced by a laser cladding process is reached in several laser passes over the substrate (two passes in the coating shown in Fig. 10). If the number of passes becomes a few hundred, then the cladding gains a third (*z*-axis in Fig. 13) dimension and can be considered a rapid prototyping process.

Table 8 Examples of 2SLD with a coating predeposited with methods other than thermal spraying

Predeposition technique	Lasing medium	Laser power density (q), kW/cm^2	Substrate composition, wt%	Final coating: Composition before coating, wt%	Final coating: Thickness, μm	Final coating: Phase composition	Laser treatment process: Substrate speed, cm/s	Laser treatment process: Overlapping	Ref
Cladding									
Screen printing	CO_2, cw	50	Low-carbon steel	Na-Ca-Al-B silicate glass	500	Amorphous to crystalline, depending on processing conditions	0.3-0.6	…	63
Paste preplacing	CO_2, cw	10-15	AISI 1045 steel	WC-Co + self-fluxing alloy (Ni-Cr-Si-B-Fe) + organic binder	1200	$Cr_{23}C_6$ and other carbides and borides	0.1-0.6	20	64
Alloying									
Physical vapor deposition	Nd:YAG, pulsed, τ = 130 ns, repetition rate 11 kHz	80×10^3 to 200×10^3	Ni	Ag, Au, Pd, Sn, Ta	0.06-0.3	Intermetallic alloys	50-600	…	65, 66
Painting of slurry	CO_2, cw	1-3 kW laser power	Ti + 6Al + 4V	Graphite with methanol		TiC		…	67
Hard phase dispersion									
Screen printing	CO_2, cw with integrator	36-130	Al99.9	TiC or TiB_2 with organic binder	120	Traces of Al_2O_3, Al, TiC, TiB_2	7.5-30	…	68

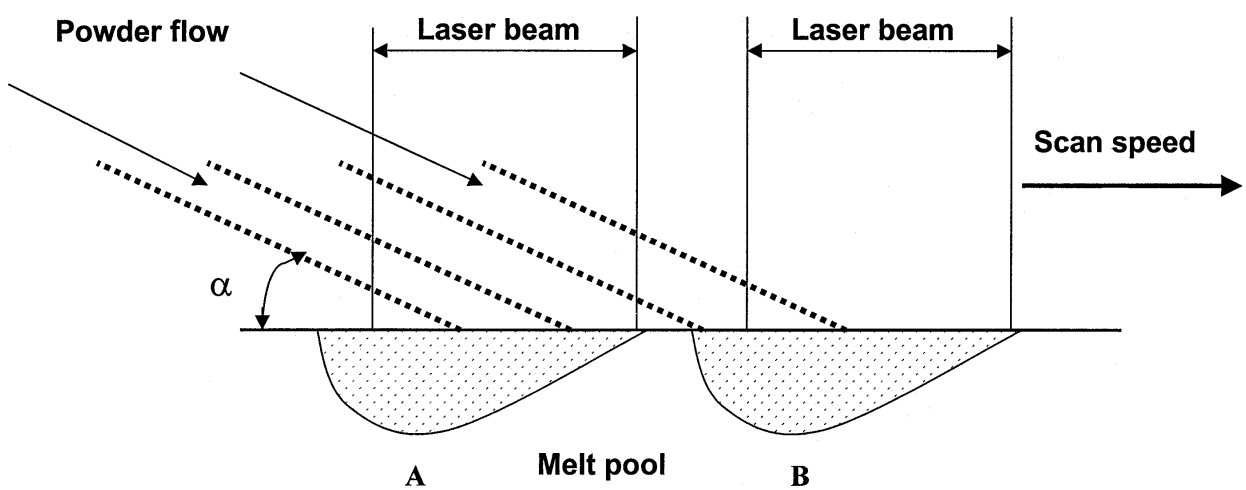

Fig. 12 The position of the powder injection spot with regard to a laser beam. A, middle of the laser beam; B, back of the laser beam. Source: Ref 55

The rapid prototyping process enables thin-walled, precisely designed metal structures with a density close to 100% (Ref 60, 61) to be obtained. The structures can be produced with the use of a few powdered components introduced through the nozzles into a laser melted pool (Fig. 14).

The thickness of the walls produced by rapid prototyping could be as small as the laser spot (from 0.1 μm to a few millimeters). The microstructure of these three-dimensional products is similar to that obtained by powder sintering. The process was applied to form shapes for stamping machines (Ref 61) and to fill cracks in damaged bearings, crankshafts, and cylinders in automotive engines (Ref 62).

3.2 Two-Step Laser Deposition

The 2SLD consists of a laser treatment of a predeposited coating (Fig. 15). The laser treatment, being a second step in a two-step laser deposition process, is easier to control than it is in the 1SLD process. The laser treatment process does not include variables related to powder injection (e.g., powder feed rate, carrier gas flow rate, angle of injection, etc.). Moreover, the predeposited coating already has a defined thickness. However, the 2SLD requires expertise in mastering two different processes.

Predeposition with Techniques Other than Thermal Spraying. A few examples of the 2SLD process with an initial coating deposited with methods other than thermal spraying are shown in Table 8. The reviewed methods belong to families (classified in Ref 69) of bulk coating deposition for thick films (painting, screen printing, and paste deposition) and atomistic coating deposition for thin films (physical vapor deposition) (PVD). The microstructure of coatings that are laser treated in the liquid phase is typical for rapidly solidified materials, and the coatings are mainly developed to resist wear.

Predeposition with Thermal Spraying. The application of a laser can improve the properties of thermally sprayed coatings. Improvements recently studied concern biomedical coatings, thermal barrier coatings, wear resistant composite coatings, corrosion resistant alloys, and wear resistant coatings engraved with a laser (anilox rolls). Most of the laser treatments correspond to the process of cladding, and only a few papers concern alloying or hard phase dispersion. Therefore, the following discussion is segmented to take into account the state of the sprayed coating at the laser processing stage (i.e.: the solid, liquid, and gaseous states).

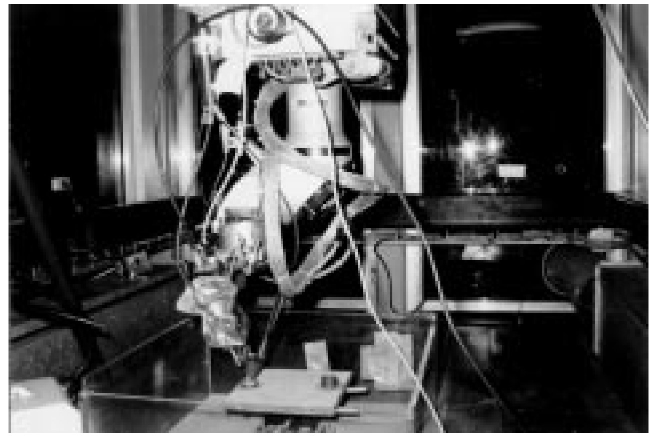

(a)

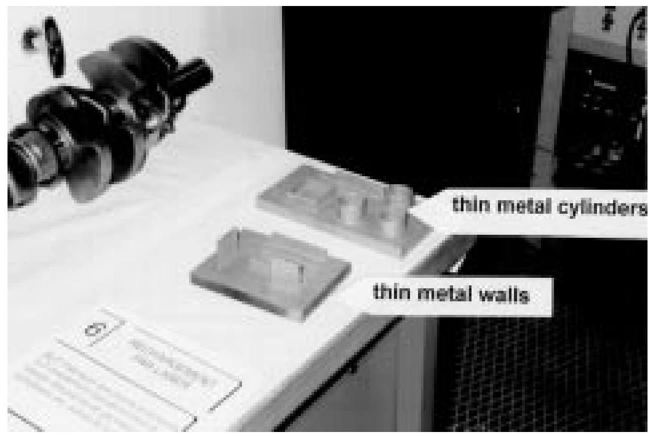

(b)

Fig. 14 Rapid prototyping. A, installation; B, examples of thin-walled metal structures produced at the laboratory CLFA, Arcueil, France

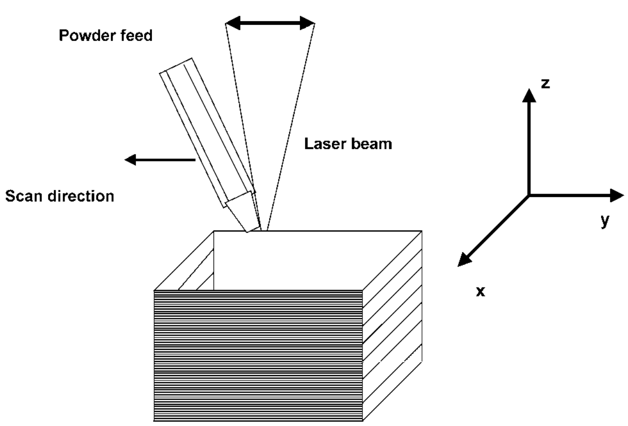

Fig. 13 Sketch of laser rapid prototyping process

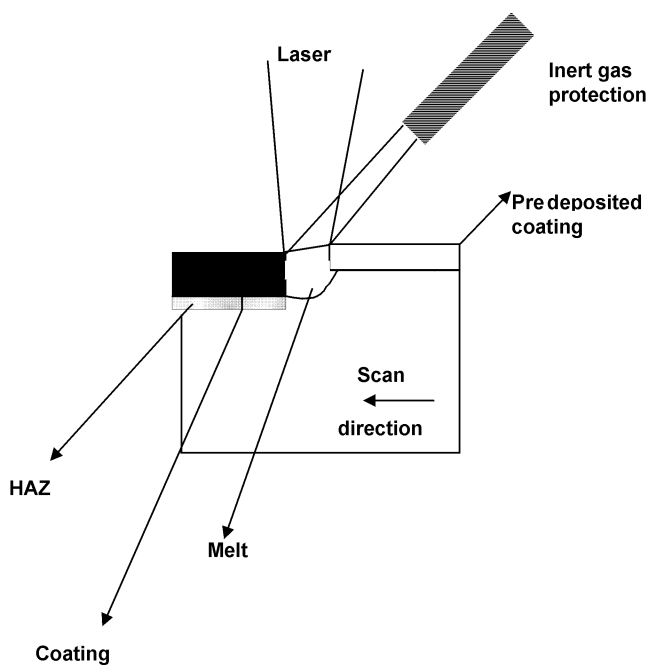

Fig. 15 Two-step laser deposition

Treatment in the solid phase has been performed for hydroxyapatite (HAp) coatings. Thermal spraying of HAp is achieved by the atmospheric plasma spraying (APS) process (Ref 70, 71) and sometimes by VPS or HVOF processing. The major problem of spraying is related to the fact that grains of HAp powder decompose in a flame at about 1550 °C (Eq 7), and the products of this decomposition, $Ca_3(PO_4)_2$ (TCP), $Ca_4P_2O_9$ (TTCP), and also CaO, are not the preferred phases from the point of view of biocompatibility.

$$Ca_{10}(PO_4)_6(OH)_2 \rightarrow 2\,\alpha\,Ca_3(PO_4)_2 + Ca_4P_2O_9 + H_2O \qquad \text{(Eq 7)}$$

Because the HAp has relatively low thermal conductivity, it is probable that the particles in the flame are liquid on their periphery and solid inside. On solidification, the low melting point oxides are known to become amorphous. Thus, the individual lamellae in the coatings are composed of many phases (Fig. 16).

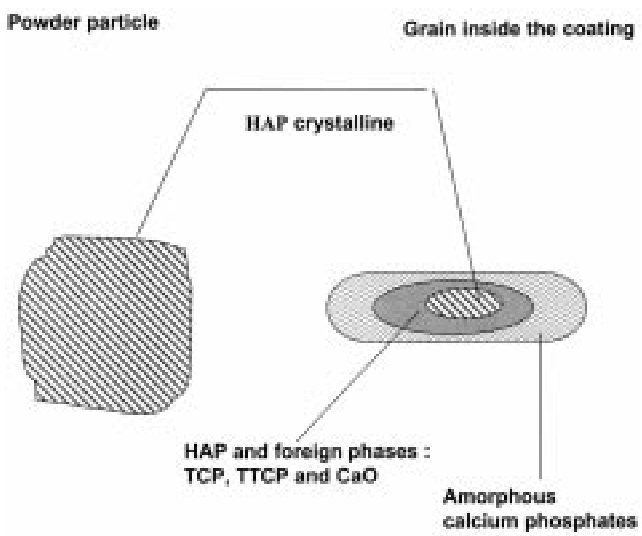

Fig. 16 Transformation of a HAp grain in a lamella inside the coating

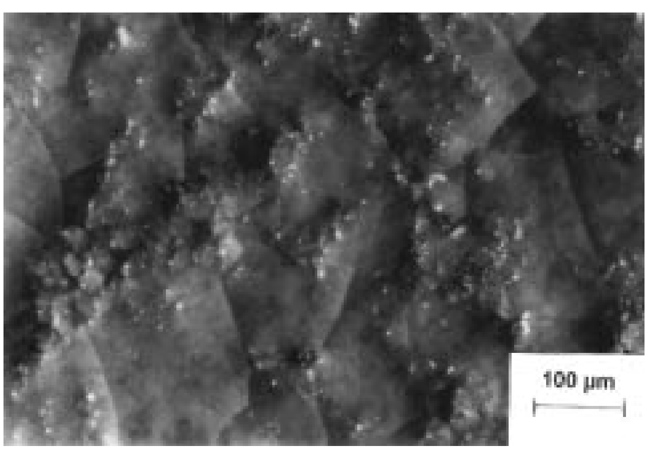

Fig. 17 Optical micrograph of the surface of HAp coating predeposited with atmospheric plasma spraying (APS) and laser treated in solid phase. The laser processing enabled the increase of crystalline HAp from 23% (as-sprayed coating) to 90%. Source: Ref 70

Laser treatment in the solid phase might enable transformation of the amorphous phase in an outer region of the HAp lamellae. The parameters of the treatment are collected in Table 9.

The laser treatment was optimized in Ref 70 and enabled the content of crystalline HAp to be restored from 23% in as-sprayed coatings to 90% (Fig. 17). The following study (Ref 71) enabled the phase content to be related to the temperature of the coating surface on laser treatment. The optimum temperature of the treatment was in the range of 800 to 1100 °C, which is well below the decomposition temperature. At these conditions, the amorphous calcium phosphates were indeed transformed to a crystalline HAp (Fig. 18).

Another example of the laser treatment in the solid phase concerns composites reinforced with carbides. The carbides are known to decompose at high temperatures. Therefore, laser treatment via a shock treatment (see section 2) at room temperature is a promising way to improve their properties. The Al + SiC coatings predeposited with HVOF were treated with LSP in Ref 73. The composites were processed with the parameters collected in Table 10.

The treatment modified the microstructure and morphology of the coatings in many ways: (a) contact between the aluminum matrix and the SiC reinforcement became closer (Fig. 19), (b) lamellae of the aluminum matrix became plastically deformed, and (c) the coating surface became smoother. However, in spite of an improved microstructure, the oscillating wear resistance of treated composites was worse than that of as-sprayed deposits. This effect was explained by the formation of structural defects at the coating surface during the laser processing.

Treatment in liquid phase is sometimes called remelting or glazing. This concept to improve the properties of sprayed coatings is only several years older than the laser itself (Ref 74). Presently, it is the most popular variation of laser treatment of thermally sprayed coatings. Many types of sprayed coatings, such as metals, alloys, and oxide ceramic, and carbide reinforced composites were reportedly processed in this fashion (Table 11).

Metals such as Ti (Ref 75, 83) and Ni (Ref 76) were laser remelted. Ayers and Schaefer (Ref 75) indicated that the laser beam quality influences the depth of the treatment. The melting of the coating is associated with an evacuation of expanding gases entrapped in closed pores, which might leave holes on the

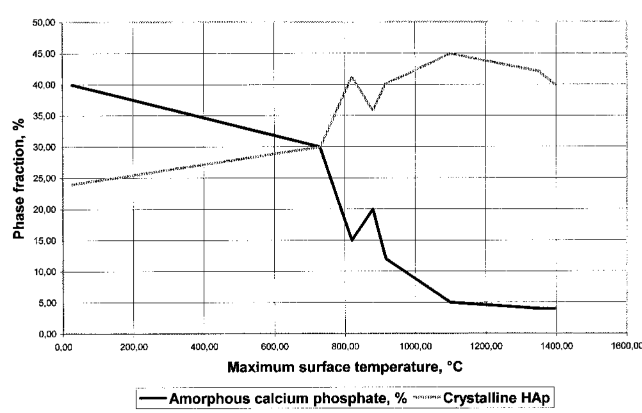

Fig. 18 Phase composition of the plasma sprayed HAp coatings submitted to a laser treatment at different processing parameters resulting in different temperatures of treatments. Source: Ref 71

coating surface. Finally, the processing parameters, such as substrate speed and laser power density, should be carefully optimized to avoid residual stresses that can relax to form cracks. Laser remelting seals the metal coatings and eliminates the post-spray porosity. A formation of 3 μm thick TiC was observed (Ref 83) in the interface of remelted titanium coating on graphite. Thus, to obtain a dense metal coating without holes on the surface, the predeposition with VPS and laser treatment in a vacuum are prerequisite. The laser remelted Ti or Ni coatings were developed to resist corrosion.

A modeling of laser remelting of VPS NARloy-Z alloy (Co + 3 wt% Ag + 0.5 wt% Zr) was analyzed with a mathematical model in Ref 84. The model enables estimation of the melting depth. Typical parameters of treatment are collected in Table 11.

The sprayed alloys can form amorphous and nanocrystallite phases of different intermetallic compounds, such as $AlNi_3$ (Ref 77) after remelting of NiCrBSi self-fluxing alloy. The laser glazing eliminated unmelted grains in the coatings and closed the open porosity that occurs frequently in sprayed deposits (Fig. 20).

The characteristics of laser glazed coatings make them useful in such applications as corrosion resistance (Hastelloy C in Ref 85, Hastelloy 6 in Ref 86, and NiCr in Ref 87), oxidation resistance at high temperatures (NiCoCrAlYTa in Ref 88), and wear resistance (CoCrAlY in Ref 78, NiCrBSi in Ref 89). An interesting technique of simultaneous VPS and CO_2 laser treatment of a phosphor bronze coating was also proposed recently (Ref 90).

As opposed to metals and alloys, laser remelted ceramic coatings are cracked on their surface (Fig. 21). Typical processing parameters of ceramic coatings are shown in Table 11. The Al_2O_3 coatings deposited by APS onto a low thermal expansion Kovar alloy was tested in Ref 79. The authors observed transformation of $\gamma + \alpha$ phases of alumina present in the sprayed coatings into α Al_2O_3 in laser remelted samples.

The alumina alloyed with titania (Al_2O_3 + 13 wt% TiO_2) transformed from $\gamma + \alpha$ alumina phases and rutile (TiO_2), present in the sprayed deposit, into α Al_2O_3 and spinel (Al_2TiO_5) in a laser remelted deposit (Ref 91). The transformation was associated with coating densification, the formation of a columnar structure in a zone remelted with the laser, an increase in micro-

Table 9 Parameters of laser treatment of atmospheric plasma sprayed calcined HAp powder

Lasing medium	Laser density (*q*), kW/cm^2	Substrate composition, wt%	Final coating: Thickness, μm	Final coating: Phase composition	Substrate speed, cm/s	Ref
Nd-YAG, τ = 2.7 ms, repetition rate = 7 Hz	Laser power = 0-400 w	Medium-carbon steel	…	…	…	72
CO_2, cw	Laser power = 10-70 w	Ti + 6Al + 4V	150	90%HAp, amorphous TCP, TTCP, CaO (Fig. 17)	0.025-2.5	70
CO_2, cw, kaleidoscope	0.52-0.68	Ti + 6Al + 4V	150	HAp, amorphous, CaP (Fig. 18)	2-5	71

Table 10 Parameters of laser shock treatment of Al + SiC composites

Spraying: Technique	Spraying: Powder composition, wt%	Laser medium	Laser power density (*q*), GW/cm^2	Substrate composition, wt%	Final coating: Thickness, μm	Final coating: Phase composition	Laser treatment process: Number of shocks in a spot	Laser treatment process: Overlapping, %	Laser treatment process: Pressure of one shock (*p*), GPa
HVOF	Al + (15-50)SiC powder blend	Nd:glass, τ = 5-20 ns, energy = 80 J	5-10	Al alloy	100-400	Al, SiC (Fig. 19)	1-2	50	4-5.5

Source: Ref 73

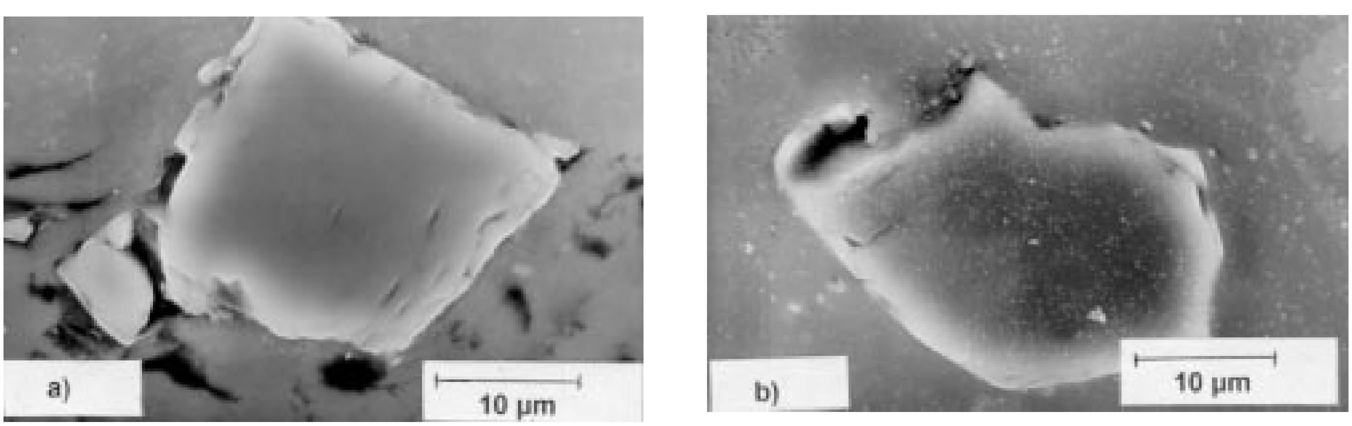

Fig. 19 SEM of the cross section of a Al + 15 SiC particulate composite (a) predeposited with HVOF and (b) laser shock treated

hardness ($HV_{0.2}$) from 950 to 2000, and an improvement of wear and corrosion resistance. Ceramics of the same composition were plasma sprayed on top of a multicoating composed of a NiAl bond layer and a NiAl + 50 wt% (Al_2O_3 + 13 wt% TiO_2) intermediate layer. The multicoating was applied onto AlSi alloy and remelted with a CO_2 cw laser (Ref 92). The samples were subsequently submitted to thermal shocks (500 °C for 5 min followed by water quenching to 10 °C). The laser treated specimen was more resistant to thermal shocks than the as-sprayed coating. The authors pointed out that the stresses generated by thermal shock testing were more easily relieved by the formation of the network cracks in the laser treated samples.

Another important thermally sprayed oxide ceramic, ZrO_2, was also the subject of many studies on laser glazing (Ref 80, 93-100). In most papers, zirconia was a part of a thermal barrier coating (TBC) system (ZrO_2, top coating; MCrAlY alloy, bond coating). The reason for interest in laser treatment results from the formation of a columnar microstructure in the sprayed deposits (Fig. 22). This type of segmented microstructure with vertical columns is typical for zirconia obtained by electron beam physical vapor deposition (EBPVD) (Ref 101) and might also be obtained by a cryogenic gas cooling during the spraying process (Ref 102). Because TBCs are submitted to intensive thermal shocks during service, the distance between the columns could increase (at heating) and decrease (at cooling) without damaging the entire TBC. Thus, the strain tolerance of the TBC having a segmented microstructure is improved. Another improvement introduced by laser glazing is the decrease of the coating roughness resulting in better aerodynamic behavior of the TBC onto turbine blades.

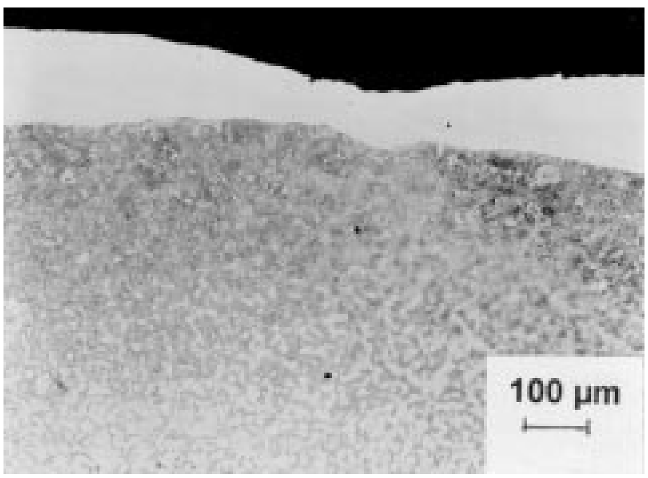

Fig. 20 Optical micrograph of the polished cross section of CoCrAlY coating deposited initially by vacuum plasma spraying (VPS) and laser remelted (see Table 11)

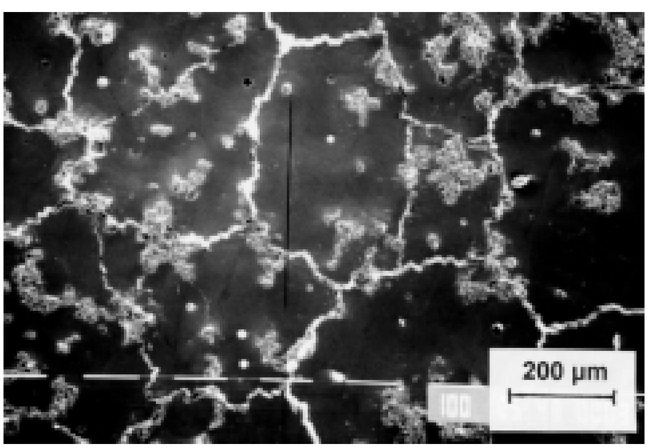

Fig. 21 SEM micrograph (secondary electrons) of the surface of Al_2O_3 coating deposited initially by APS and laser remelted (see Table 11)

The density of segments was reportedly smaller when a pulsed (instead of cw) CO_2 laser was applied (Ref 97). The microstructure of the laser remelted zirconia depended on the percentage of yttria stabilizer in the powder used to spray. At 8 wt%, the structure was mainly tetragonal nontransformable (t′) and cubic (c) (Ref 95), and at 12 wt%, it was cubic (Ref 98). At 20 wt%, the structure was cubic again (Ref 94). The grains in the laser treated coating were reported (Ref 97) to be cellular at a laser specific energy less than 1 J/mm^2 and dendritic at the higher energies. The thermal shock behavior of laser remelted TBC compared to as-sprayed coatings indicated no improvement in the initial study (Ref 93) and a fourfold improvement in a more recent study (Ref 98). The corrosion resistance of a glazed specimen can be improved by better sealing of the coatings, and two ideas were proposed. Chen et al. (Ref 99) initially remelted the coating to a depth of about 100 μm and applied a zirconia suspension to the coating surface, followed by treatment with lower laser power density to the depth of 50 μm. Troczynski et al. (Ref 80) employed sol gel sealing with the laser treatment.

Laser treatment of MMC (mainly with carbide reinforcement) should improve contacts between the reinforcement and the matrix and reduce/eliminate the porosity of the metal matrix. Consequently, the wear resistance of the composites is expected to increase. The main problem of the treatment is related to the

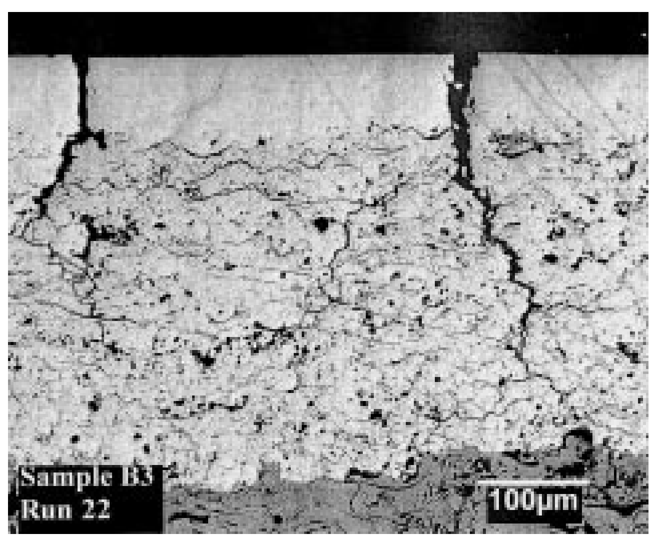

Fig. 22 SEM micrograph (backscattered electrons) of the polished cross section of a thermal barrier coating (TBC) composed of MoCrAlY bond coating and ZrO_2 + 8 wt% Y_2O_3 ceramic laser remelted (see Table 11)

melting of the carbide reinforcement being associated with possible decomposition and the decrease in hardness or the rounding of the blocky carbide particulate that does not favor wear resistance. The first solution by laser shock treatment was presented previously.

Another solution is a laser remelting of MMCs in a way that keeps carbide reinforcement solid and melts the metal matrix. This solution is possible because the melting point of metals is usually much lower than that of carbides. It demands, however, careful control of the laser treatment temperature. This approach was adopted by the authors of Ref 81 who applied a very porous powder of a composition (Fe + 13 wt% Cr) + 55 wt% TiC prepared with a self-propagating high-temperature synthesis (SHS) method with APS technique onto steel substrate. The sprayed coating was very porous (Fig. 23a), and it was submitted to a laser glazing.

The alloy matrix melts at 1538 °C, and, at the other extreme of temperature, a eutectic reaction of the titanium carbide reinforcement with the graphite can take place at 2776 °C, as in the following:

Table 11 Parameters of laser remelting of selected thermally sprayed coatings

Spraying			Laser	Substrate	Final coating		Laser treatment process			
Technique	Powder composition, wt%	Lasing medium	power density (q), kW/cm^2	composition, wt%	Thickness, μm	Phase composition	Substrate speed, cm/s	Atmosphere	Overlapping, %	Ref
Metals										
VPS	Ti	CO_2, cw	1300	1020 steel	300-380	Ti	30	He, vacuum	…	75
APS	Ni	CO_2, pulsed, τ = 40 μs	8000	Steel	50-300	…	…	…	…	76
Alloys										
APS	Self fluxing alloy: Ni + 11Cr + 11Fe + 1.5Si + 1B	CO_2, cw	36	Al + 8Si + 1Cu + 0.5Mg	400	Al, Al_3Ni, AlNi, Al_3Ni_2, …	1	Ar	…	77
VPS	Co + 17Cr + 12Al + 0.5Y	CO_2, cw	7.5	Mild steel St38b	100-150	Fig. 20	12-22		66	78
Ceramics										
APS	αAl_2O_3	CO_2, cw	13	Kovar, Fe + 29Ni + 17Co + 0.4Mn	400-500	γAl_2O_3 (Fig. 21)	1.2	Air, Ar	70	79
	$ZrO_2 + 8Y_2O_3$	CO_2, cw	3-7	Ni alloy	380	Fig. 22	20	…	…	80
Composites										
APS	Fe13Cr + 55wt%TiC by SHS method	CO_2, cw, beam shaped with kaleidoscope	8	Steel St38	200 or 400	TiC, Cr, Fe_2C	0.25-1	…	1 pass	81
	WC + 17Co	CO_2, cw, beam shaped with integrator	Energy density, 300-2300 J/cm^2	Steel AISI 1043	…	Dendritic grains	0.83	Ar	25	82

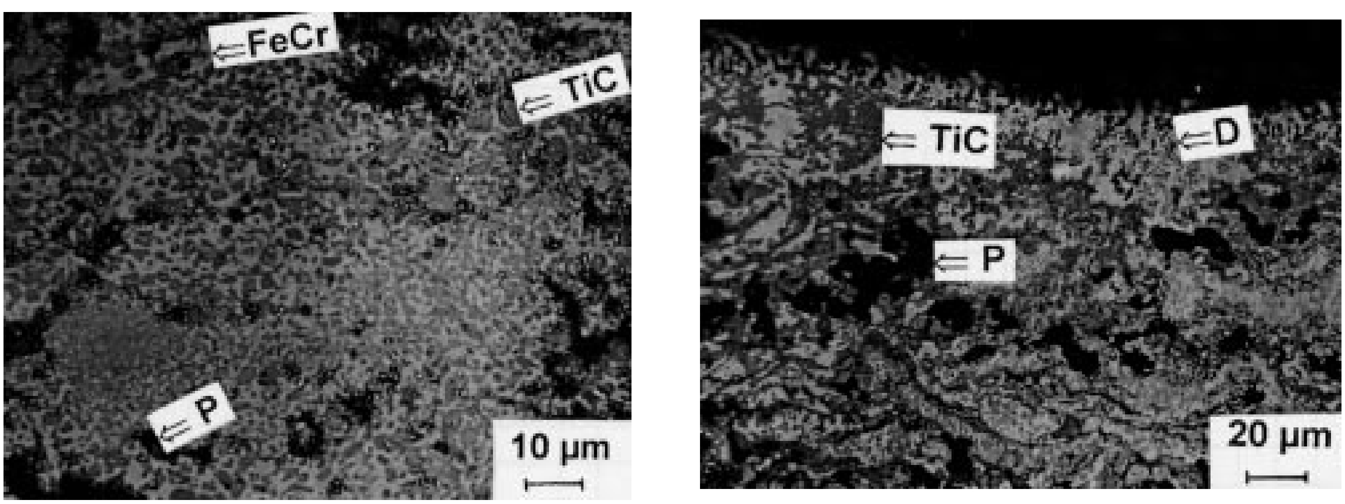

(a) (b)

Fig. 23 Optical micrograph of the polished cross section of FeCr-TiC coatings (a) as sprayed and (b) laser glazed. The microstructure features are TiC, grains of TiC; P, pore; D, dendrite; and FeCr, matrix.

$$TiC + C \leftrightarrow L \quad \text{(Eq 8)}$$

On solidification from the melt, the formation of solid solutions of α Ti, β Ti, and/or Ti_2C is possible. Consequently, to melt the matrix and keep the reinforcement solid, the temperature of the coating surface at laser glazing was maintained at about 2000 °C. Post-processing in these conditions enabled the densification of the coating at the surface (Fig. 23b) without the decomposition of titanium carbide (Fig. 24). The wear resistance of laser glazed coatings was more improved than that of as-sprayed coatings.

Treatment in gaseous phase mainly concerns laser engraving, which is part of the manufacturing of anilox rolls reviewed in Ref 103. The rolls are used to transport a precise quantity of ink in flexographic printing machines. The actual technology of the rolls includes the spraying of Cr_2O_3 coating with APS and the subsequent laser engraving of the cells. The typical cell line density is a few hundred lines on one centimeter.

Recent developments in this field concern the research of alternative coatings to Cr_2O_3 ceramics and research to improve the production quality of laser engraving. Beczkowiak et al. (Ref 104) investigated the laser engraving of Al_2O_3, TiO_2, Al_2TiO_5, and Al_2O_3 alloyed with different contents of TiO_2 coatings applied with the APS technique. These authors found that the industrial laser engraving of Al_2TiO_5 and Al_2O_3 + 60 wt% TiO_2 coatings produces cells that are quite similar to those engraved in Cr_2O_3 coatings. The laser engraving process was also simulated with a mathematical model (Ref 105, 106). The model verified that, using the same laser engraving parameters, the thickness of a liquid phase for Al_2O_3 and Al_2TiO_5 coatings is smaller than that for Cr_2O_3 coating (Fig. 25).

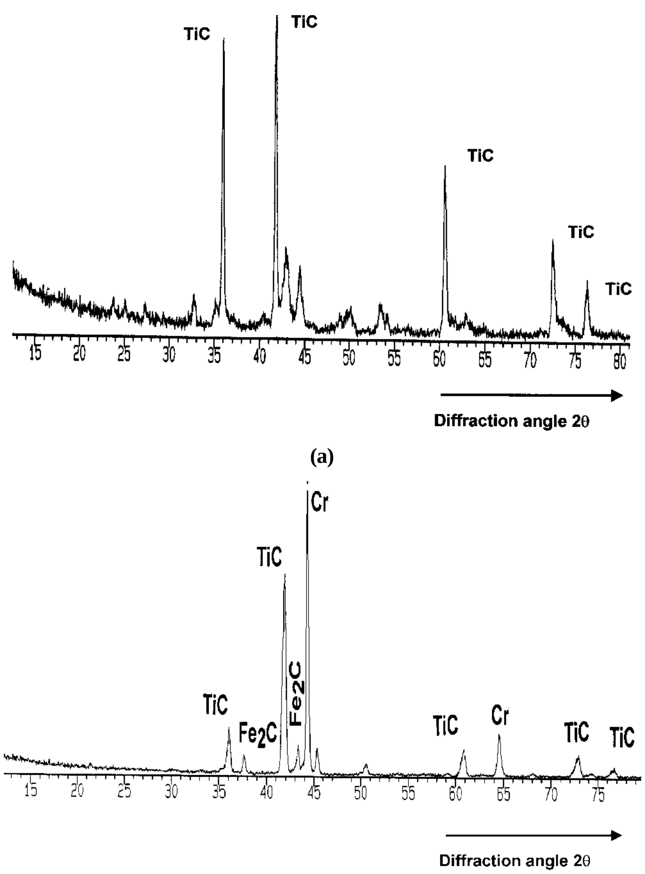

Fig. 24 XRD of (a) as sprayed and (b) laser glazed FeCr-TiC composites

Because liquid ceramics can be blown out of the cell and deteriorate the coating quality (overflow effect), anilox rolls of better quality can be produced by applying alumina and alumina-titania spinel. However, many further studies are necessary to convince roll manufacturers and their customers to replace chromia with these ceramics. On the other hand, the manufacturers of the installations to engrave the coatings have introduced sophisticated optical systems, such as the new anilox technology of ZED Instruments (Ref 107). This technology enables, for example, deflection of the laser beam across the surface of the engraved roll to obtain higher quality of engraving at a high density of cells or double engraving of the same cell to reach higher depth of cells. The industrial tendency is toward an increase of the density of the cells (fine pattern anilox rolls). Because the engraved cell diameter is physically limited by the laser emission wavelength CO_2 (Eq 3), it is impossible to obtain a cell of diameter less than 10 µm with a currently used CO_2 laser. Therefore, the solid state lasers (e.g., Nd:YAG) having shorter wavelength are increasingly tested in anilox roll production (Ref 108, 109).

4. Conclusions

- Thick coatings of metals, alloys, and ceramics can be deposited with high power lasers.
- The metal and alloy coatings are frequently deposited in one step by the use of powder injection to the melt pool.

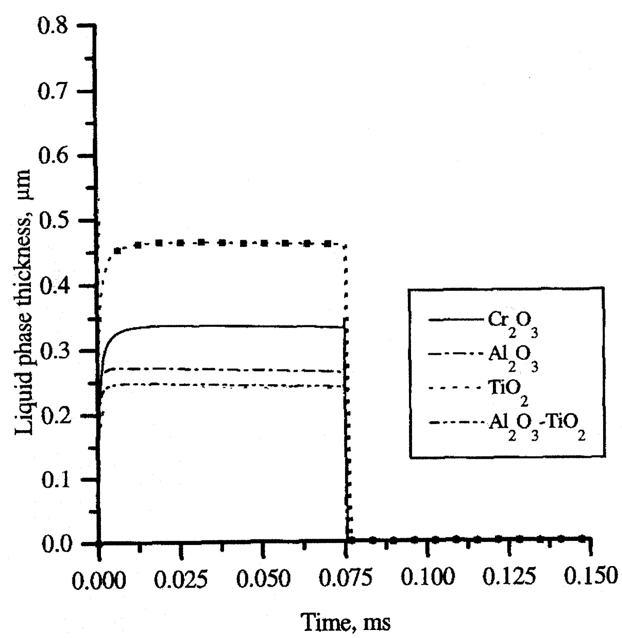

Fig. 25 Calculated liquid phase thickness in the cells engraved in different ceramic coatings using the laser power density $q = 2.5$ MW/cm^2 and a pulse length $\tau = 75$ µs. The calculations for titania were made using the parameters thermal conductivity = 2 W/(m · K) and thermal diffusivity = 5×10^{-7} m^2/s.

- A new technology related to this deposition technique is rapid prototyping.
- Another technique consists of placing the initial coating onto substrate and subsequent laser treatment (two-step laser deposition). This method was used to improve properties of thermally sprayed metals, alloys, composites, and ceramics applied as biomedical coatings, thermal barrier coatings, wear resistant coatings, corrosion resistant coatings, and wear resistant coatings engraved with a laser (anilox rolls).
- Future research should be focused on better control of the process and better understanding of the physical phenomena occurring at laser treatment, such as injection of solid particles in a melt pool or solidification of the coating.

Acknowledgment

The laser treatments of sprayed coatings were made in the French laser centers CALFA in Béthune (Dr. A. Deffontaine) and CLFA in Arcueil (Dr. R. Fabbro) and in the Italian laboratory ITIA-CNR in Milan (Dr. L. Covelli). The studies on laser treatments of CoCrAlY and the composite coatings were made in collaboration with Professor B. Wielage (University of Chemnitz, Germany) and financed by a French-German Procope program. The laser treated TBC were studied in collaboration with A/Professor T. Troczynski of University of British Columbia, Vancouver, Canada. The modeling of laser treatment was realized in collaboration of Professor I. Smurov of University of Saint Etienne (France).

References

1. L. Pawlowski, *The Science and Engineering of Thermal Spray Coatings,* John Wiley & Sons, Ltd., Chichester, England, 1995
2. W.M. Steen, *Laser Material Processing,* Springer-Verlag, Berlin, Germany, 1991
3. C. Belouet, "Thin Film Growth by the Pulsed Laser-Deposition (PLD) Technique: Towards Applications?" Paper SIII-4: IL06, presented at 9th Cimetec, (Florence, Italy), Techna, 14-19 June 1998
4. M.G. Hocking, V. Vasantasree, and P. S. Sidky, *Metallic & Ceramic Coatings,* Longman, Burnt Mill, England, 1989
5. A.E. Siegman, *Lasers,* University Science Book, Sausalito, CA, 1986
6. G. Herziger and P. Loosen, *Werkstoffbearbeitung mit Laserstrahlung,* Carl Hanser Verlag, München, 1993
7. H. Rapinel, R. Pitt, and L. Pawlowski, "Industrial Placement Report," ZED Instruments/University Artois, 1996
8. L.R. Migliore, Heat Treating with Lasers, *Adv. Mater. Process.,* Vol 154 (No. 2), 1998, p H25-H29
9. M.A. Ordal, L.L. Long, R.J. Bell, S.E. Bell, R.R. Bell, R.W. Alexander, Jr., and C.A. Ward, Optical Properties of the Metals Al, Co, Cu, Au, Fe, Pb, Ni, Pd, Pt, Ag, Ti, and W in the Infrared and Far Infrared, *Appl. Optics,* Vol 22, 1983, p 1099-1119
10. *American Institute of Physics Handbook,* 3rd ed., McGraw-Hill Publishing Co., 1972
11. M. von Allmen, Coupling of Beam Energy to Solids, *Laser and Electron Beam Processing of Materials,* P.S. Peary, Ed., Academic Press, 1980, p 6-19
12. M. Bass, Laser Heating of Solids, *Physical Processes in Laser –Materials Interactions,* M. Bertolotti, Ed., Plenum Press, 1983, p 77-115
13. H.S. Carslaw and J.C. Jaeger, *Conduction of Heat in Solids,* 2nd ed., Oxford University Press, London, 1959
14. T. Witke and A. Lenk, Vergleich der Plasmaparameter Erzeugt mit Verschiedenen Lasern, *6th European Conference on Laser Treatment of Materials, ECLAT'96,* Vol 1, F. Dausinger, H.W. Bergmann, and J. Sigel, Ed., AWT, Stuttgart, Germany, 1996, p 567-574
15. C.B. Dane, L.A. Hackel, J. Daly, and J. Harrison, Shot Peening with Lasers, *Adv. Mater. Process.,* Vol 153 (No. 5), 1998, p 37-38
16. N.C. Anderholm, Laser Generated Stress Waves, *Appl. Phys. Lett.,* Vol 16 (No. 3), 1970, p 113-115
17. P. Peyre, R. Fabbro, L. Berthe, and C. Dubouchet, Laser Shock Processing of Materials, Physical Processes Involved and Examples of Applications, *J. Laser Appl.,* Vol 8 (No. 3), 1996, p 135-141
18. J.E. Masse and G. Barreau, Laser Generation of Stress Waves in Metal, *Surf. Coat. Technol.,* Vol 70, 1995, p 231-234
19. C. Keusch, G. Hintz, R. Tkotz, M. Negendanck, J. Christiansen, H.W. Bergmann, K. Eisner, and K. Schutte, Shock Hardening, A Novel Technique for Materials Processing, *6th European Conference on Laser Treatment of Materials, ECLAT'96,* Vol 1, F. Dausinger, H.W. Bergmann, and J. Sigel, Ed., AWT, Stuttgart, Germany, 1996, p 439-446
20. D. Devaux, R. Fabbro, and J. Virmont, Generation of Shock Waves by Laser-Matter Interaction in Confined Geometries, *J. Phys. (France) IV, colloque C7,* Vol 1, 1991, p 179-182
21. T.R. Tucker, A.H. Clauer, I.G. Wright, and J.T. Stropki, Laser-Processed Composite Metal Cladding for Slurry Erosion Resistance, *Thin Solid Films,* Vol 117, 1984, p 73-84
22. S. Nowotny, B. Grünewald, W. Reitzenstein, and H. Hügel, Systemtechnik zum Laserstrahl—Präzisionbeschichten, *6th European Conference on Laser Treatment of Materials, ECLAT'96,* Vol 1, F. Dausinger, H.W. Bergmann, and J. Sigel, Ed., AWT, Stuttgart, Germany, 1996, p 383-390
23. H. Kindler, R. Volz, and M. Huonker, Ein Neues Verfahren zum Laserbeschichten, *6th European Conference on Laser Treatment of Materials, ECLAT'96,* Vol 1, F. Dausinger, H.W. Bergmann, and J. Sigel, Ed., AWT, Stuttgart, Germany, 1996, p 447-454
24. F. Mériaudeau, F. Truchetet, and C. Dumont, High Speed Photography Applied to Laser Cladding Process, *Proc. of the SPIE—The International Society for Optical Engineering,* Vol 2869, 1997, p 994-1003
25. J.M. Jouvard, D. Grevey, F. Lemoine, and A.B. Vannes, Dépôts par Projection de Poudre dans un Faisceau Laser Nd:YAG: cas de Faibles Puissances, *J. Phys. (France) III,* Vol 7, 1997, p 2265-2274
26. A. Frenk, M. Vandyoussefi, J.-D. Wagnière, A. Zryd, and W. Kurz, Analysis of the Laser-Cladding Process for Stellite on Steel, *Metall. Mater. Trans. B,* Vol 28, 1997, p 507-508
27. Y. Li and J. Ma, Study on Overlapping in the Laser Cladding Process, *Surf. Coat. Technol.,* Vol 90, 1997, p 1-5
28. St. Nowotny, J. Shen, and F. Dausinger, Verschleiβschutz durch Auftragschweiβen von Stellit 21 mit CO_2 Laser, *Laser und Optoelektronik,* Vol 21 (No 6), 1991, p 50-54
29. A. Adamski, R. Bamola, and L. Hultman, "HVOF Spraying and Laser Processing of Waspaloy Thick Films," Paper 92-GT-368, presented at 37th ASME International Gas Turbine Aeroengine Congress and Exposition, (Cologne, Germany), 1-4 June 1992, American Society of Mechanical Engineers
30. J.M. Pelletier, E. Sauger, Y. Gachon, and A.B. Vannes, Hadfield Steel Layers Manufactured by Laser Cladding: Mechanical and Tribological Properties, *6th European Conference on Laser Treatment* of Materials, ECLAT'96, Vol 1, F. Dausinger, H.W. Bergmann, and J. Sigel, Ed., AWT, Stuttgart, Germany, 1996, p 329-336
31. M. Cadenas, E. Fernandez, M. R. Fernandez, and J.M. Cuetos, Laser Cladding of Tungsten Carbide Powder, *Surface Treatment '97,* M.H. Aliabadi and C.A. Berbbia, Ed., Computational Mechanics Publications, Southampton, U.K., 1997, p 241-256
32. J.J. Blechet, Direction Générale d'Armement, F-94114 Arcueil, France, personal communication, 1997
33. J.M. Yellup, Laser Cladding Using the Powder Blowing Technique, *Surf. Coat. Technol.,* Vol 71, 1995, p 121-128

Peer Reviewed

34. M.A. Anjos, R. Vilar, and Y.Y. Qiu, Laser Cladding of ASTM S 31254 Stainless Steel on a Plain Carbon Steel Substrate, *Surf. Coat. Technol.*, Vol 92, 1997, p 142-149
35. J. de Damborena, V. Lopez, and A.J. Vazquez, Improving High-Temperature Oxidation of Incoloy 800H by Laser Cladding, *Surf. Coat. Technol.*, Vol 70, 1994, p 107-113
36. A. Kagawa and Y. Ohta, Wear Resistance of Laser Clad Chromium Carbide Surface Layers, *Mater. Sci. Technol.*, Vol 11, 1995, p 515-519
37. S. Nowotny, A. Müller, A. Techel, and S. Schädlich, Mechanische Eigenschaften von Laser-Beschichtungen aus WC-Verstärkten Hartlegierungen, *Thermische Spritzkonferenz TS96*, DVS-Berichte Band 175, DVS-Verlag GmbH, 1996, p 155-159
38. J. Kelly, K. Nagarathnam, and J. Mazumder, Laser Cladding of Wear Resistant Coatings on Cast Al-Si Alloys, *ICALEO'96*, F. DiPietro and F. Kuepper, Ed., Laser Institute of America, Vol 82, 1996, p 144-153
39. S. Nowotny and A. Müller, Lasertechnologien für Keramische Beschichtungen, *Status-Seminar Keramische Schichten*, Fortschrittsberichte der Deutschen Keramischen Gesellschaft, Band 10 (Heft 2), 1995, p 47-57
40. Y.T. Pei, J.H. Ouyang, and T.C. Lei, Laser Cladding of ZrO_2-(Ni Alloy) Composite Coating, *Surf. Coat. Technol.*, Vol 81, 1996, p 131-135
41. X.B. Zhou and J.Th.M. De Hosson, Al/γ-Al_2O_3 Interface in Laser Coated Aluminum Alloys, *Scr. Metall. Mater.*, Vol 33 (No 8), 1995, p 1345-1351
42. J.H. Abboud, R.D. Rawlings, and D.R.F. West, Functionally Graded Nickel Aluminide and Iron Aluminide Coatings Produced Via Laser Cladding, *J. Mater. Sci.*, Vol 30, 1995, p 5931-5938
43. A. Fischer and G. Lensch, Technical Application of Laser Surface Treatment—Hardening, Alloying, Cladding, *6th European Conference on Laser Treatment of Materials, ECLAT'96*, Vol 1, F. Dausinger, H.W. Bergmann, and J. Sigel, Ed., AWT, Stuttgart, Germany, 1996, p 399-405
44. J.A. Folkes, Developments in Laser Surface Modification and Coating, *Surf. Coat. Technol.*, Vol 63, 1994, p 65-71
45. G.E. Possin, H.G. Parks, and S.W. Chiang, Convection in Pulsed Laser Formed Melts, *Laser and Electron-Beam Solid Interactions and Materials Processing*, J.F. Gibbons, L.D. Hess, and T.W. Sigmon, Ed., North-Holland, 1981, p 73-80
46. S. Brenner, S. Bonβ, R. Franke, I. Haase, and H.-J. Scheibe, Mechanical Properties of Laser Gas Alloyed Ti6Al4V, *6th European Conference on Laser Treatment of Materials, ECLAT'96*, Vol 1, F. Dausinger, H.W. Bergmann, and J. Sigel, Ed., AWT, Stuttgart, Germany, 1996, p 477-484
47. A. Almeida, M. Anjos, R. Vilar, R. Li, M.G.S. Fereira, W.M. Steen, and K.G. Watkins, Laser Alloying of Aluminum Alloys with Chromium, *Surf. Coat. Technol.*, Vol 70, 1995, p 221-229
48. P.A. Carvalho and R. Vilar, Laser Alloying of Zinc with Aluminum: Solidification Structures, *Surf. Coat. Technol.*, Vol 91, 1997, p 158-166
49. M. Ignatiev, E. Kovalev, I. Melekhin, I. Yu. Smurov, and S. Sturlese, Investigation of the Hardening of a Titanium Alloy by Laser Nitriding, *Wear*, Vol 166, 1993, p 233-236
50. C. Gerdes, A. Karimi, and H.W. Bieler, Water Droplet Erosion and Microstructure of Laser-Nitrided Ti-6Al-4V, *Wear*, Vol 186-187, 1995, p 368-374
51. R. Galun, A. Weisheit, and B.L. Mordike, Surface Alloying of Magnesium Base Alloys with High Power CO_2-Laser, *Proc. of the SPIE—The International Society for Optical Engineering*, Vol 3092, 1997, p 744-747
52. M.A. Anjos, R. Vilar, R. Li, M.G. Ferreira, W.M. Steen, and K. Watkins, Fe-Cr-Ni-Mo-C Alloys Produced by Laser Surface Alloying, *Surf. Coat. Technol.*, Vol 70, 1995, p 235-242
53. R.J. Schaefer, T.R. Tucker, and J.D. Ayers, Laser Surface Melting with Carbide Particle Injection, *Laser and Electron-Beam Processing of Materials*, C.W. White and P.S. Peercy, Ed., Academic Press, 1980, p 754-759
54. J.D. Ayers, R.J. Schaefer, and W.P. Robey, A Laser Processing Technique for Improving the Wear Resistance of Metals, *J. Met.*, Aug 1980, p 19-23
55. A.B. Kloosterman and J.Th.M. De Hosson, Ceramic Particle Injection during Laser Treatment of Titanium, *Surface Treatment '97*, M.H. Aliabadi and C.A. Berbbia, Ed., Computational Mechanics Publications, Southampton, U.K., 1997, p 286-294
56. C. Hu, H. Xin, and T.N. Baker, Laser Processing of an Aluminum AA 6061 Alloy Involving Injection of SiC Particulate, *J. Mater. Sci.*, Vol 30, 1995, p 5985-5990
57. K.P. Cooper and P. Slebodnick, Recent Developments in Laser Melt/Particle Injection Processing, *Laser Materials Processing, ICALEO'88*, G. Buck, Ed., Springer Verlag, 1989, p 3-16
58. F. Hlawka, G.Q. Song, and A. Cornet, Utilisation de Rayons X pour l'étude de Traitements de Surface Laser, *J. Phys. (France) IV, colloque C4*, Vol 6, 1996, p 123-126
59. A. Gasser, K. Wissenbach, E. Hoffmann, G. Schulte, and E. Beyer, Oberflächenbehandlung mit Zusatzwerkstoffen, *6th European Conference on Laser Treatment of Materials, ECLAT'96*, Vol 1, F. Dausinger, H.W. Bergmann, and J. Sigel, Ed., AWT, Stuttgart, Germany, 1996, p 287-298
60. E. Hoffmann, G. Backes, A. Gasser, E.W. Kreutz, R. Stromeyer, and K. Wissenbach, Prozeβüberwachung durch Temperaturregelung beim Generieren mit CO_2—Laserstrahlung, *Laser und Optoelektronik*, Vol 28 (No. 3), 1996, p 59-67
61. A. Gebhardt, *Rapid Prototyping*, Hanser Verlag, München, 1996
62. O. Graydon, Jets of Molten Metal Make Industrial Parts, *Opt. Lasers Eng.*, Feb 1998, p 33-35
63. Y. Jianquing, W. Maocai, and W. Weitao, Laser Clad Glass Coating on Carbon Steel, *Surf. Coat. Technol.*, Vol 64, 1994, p 34-40
64. P.Z. Wang, J.X. Qu, and H.S. Shao, Cemented Carbide Reinforced Nickel-Based Alloy Coating by Laser Cladding and the Wear Characteristics, *Mater. Des.*, Vol 17 (No. 5/6), 1996, p 289-296
65. C.W. Draper, C.M. Preece, and D.C. Jacobson, Laser Alloying of Deposited Metal Films on Nickel, *Laser and Electron-Beam Processing of Materials*, C.W. White and P.S. Peercy, Ed., Academic Press, 1980, p 721-727
66. C.W. Draper, J.M. Gibson, D.C. Jacobson, J.M. Poate, S.M. Shin, and J.M. Rigsbee, The Microstructure of Laser Alloyed Ni-Ta Surface Layers, *J. Mater. Sci.*, Vol 20, 1985, p 2303-2312
67. A. Bharti, D.B. Goel, and R. Sivakumar, A Study in Laser Surface Alloying of Titanium Alloys, *Laser Materials Processing, ICALEO'88*, G. Buck, Ed., Springer Verlag, 1989, p 42-51
68. D. Fischer, W. Löschau, and W. Reitzenstein, Mit Laser erzeugte grobkörnige Hartstoff-Dispersionschichten auf Aluminum—Legierung zum Verschleiβschutz, *6th European Conference on Laser Treatment of Materials, ECLAT'96*, Vol 1, F. Dausinger, H.W. Bergmann, and J. Sigel, Ed., AWT, Stuttgart, Germany, 1996, p 455-460
69. R.F. Bunshah, Ed., *Deposition Technologies for Films and Coatings*, Noyes Publications, 1982
70. L. Pawlowski, H. Rapinel, F. Tourenne, and M. Jeandin, Traitement Laser des Dépôts Plasma d'Hydroxyapatite, *Galvano-Organo-Trait. Surf.*, Vol 676, 1997, p 433-437
71. X. Ranz, L. Pawlowski, L. Sabatier, R. Fabbro, and T. Aslanian, Phases Transformation in Laser Treated Hydroxyapatite Coatings, *Proc. 15th International Thermal Spray Conf.*, C. Coddet, Ed., ASM International, 1998, p 1343-1349
72. K.A. Khor and P. Cheang, Laser Post-Treatment of Thermally Sprayed Hydroxyapatite Coatings, *Thermal Spray Industrial Applications*, C.C. Berndt and S. Sampath, Ed., ASM International, 1994, p 153-157

73. T. Schnick, S. Tondu, P. Peyre, L. Pawlowski, S. Steinhäuser, B. Wielage, U. Hofmann, and E. Bartnicki, Laser Shock Processing of Al-SiC Composite Coatings, *J. Therm. Spray Technol.,* Vol 8 (No. 2), 1999
74. H.S. Ingham, Flame Spraying Employing Laser Heating, U.S. Patent 3,310,423, March 1967
75. J.D. Ayers and R.J. Schaefer, Consolidation of Plasma Sprayed Coatings by Laser Remelting, *Proc. of SPIE—The International Society for Optical Engineering,* Vol 198, 1979, p 57-64
76. S. Dallaire and P. Cielo, Pulsed Laser Treatment of Plasma Sprayed Coatings, *Metall. Trans. B,* Vol 13, 1982, p 479-483
77. G.Y. Liang and T.T. Wong, Microstructure and Character of Laser Remelting of Plasma Sprayed Coating (Ni-Cr-B-Si) on Al-Si Alloy, *Surf. Coat. Technol.,* Vol 89, 1997, p 121-126
78. B. Wielage, S. Steinhäuser, L. Pawlowski, I. Smurov, and L. Covelli, Laser Treatment of Vacuum Plasma Sprayed CoCrAlY Alloy, *Surface Modification Technologies XI,* T.S. Sudarshan, M. Jeandin, and K.A. Khor, Ed., The Institute of Materials, London, 1998, p 687-698
79. A. Gorecka-Drzazga, L. Golonka, L. Pawlowski, and P. Fauchais, Application of the Plasma Spraying Process to the Production of Metal-Ceramics Substrates for Hybrid Electronics, *Revue Internationale des Hautes Températures et des Refractaires,* Vol 21, 1984, p 153-165
80. T. Troczynski, L. Pawlowski, N. Third, L. Covelli, and I. Smurov, Physico-Chemical Treatment of Zirconia Coatings for Thermal Barriers, *Proc. 15th International Thermal Spray Conf.,* C. Coddet, Ed., ASM International, 1998, p 1337-1342.
81. S. Tondu, T. Schnick, L. Pawlowski, B. Wielage, S. Steinhäuser, and L. Sabatier, "Laser Glazing of FeCr-TiC Composite Coatings," Paper SIII-2: L08, presented at 9th Cimtec (Florence, Italy), Techna, 14-19 June 1998
82. J. Mateos, J.M. Cuetos, E. Fernandez, and M. Cadenas, Effect of Laser Treatment on Tungsten Carbide Coatings, *Surface Treatment '97,* M.H. Aliabadi and C.A. Berbbia, Ed., Computational Mechanics Publications, Southampton, U.K., 1997, p 239-246
83. R.J. Pangborn and D.R. Beaman, Laser Glazing of Sprayed Metal Coatings, *J. Appl. Phys.,* Vol 51, 1980, p 5992-5993
84. J. Singh, B.N. Bhat, R. Poorman, A. Kar, and J. Mazumder, Laser Glazing of Vacuum Plasma Coated NARloy-Z, *Surf. Coat. Technol.,* Vol 79, 1996, p 35-49
85. S. Dallaire and P. Cielo, Pulsed Laser Glazing, *Thin Solid Films,* Vol 108, 1983, p 19-27
86. M.L. Capp and J.M. Rigsbee, Laser Processing of Plasma-Sprayed Coatings, *Mater. Sci. Eng.,* Vol 62, 1984, p 49-56
87. H. Bhat, H. Herman, and R.J. Coyle, Laser Processing of Plasma Sprayed NiCr Coatings, *Laser in Materials Processing,* TMS-AIME, Warrendale, PA, 1983, p 176-183
88. R. Streiff, M. Pons, and P. Mazars, Laser Induced Microstructural Modifications in a Vacuum Plasma Sprayed NiCoCrAlYTa Coating, *Surf. Coat. Technol.,* Vol 32, 1987, p 85-95
89. T.T. Wong and G.Y. Liang, Formation and Crystallization of Amorphous Structure in the Laser-Cladding Plasma Sprayed Coating of Al-Si Alloy, *Mater. Charact.,* Vol 38, 1997, p 85-89
90. S. Alam, S. Sasaki, H. Shimura, Y. Kawakami, and M.A. Hassan, Tribological and Microstructural Investigations of Bronze Coating by Laser and Plasma Hybrid Spraying Technique, *Surface Modification Technologies X,* T.S. Sudarshan, K.A. Khor, and M. Jeandin, Ed., The Institute of Materials, 1997, p 918-926
91. W. Aihua, T. Zengyi, Z. Beidi, F. Jiangmin, M. Xianyao, D. Shijun, and C. Xudong, Laser Modification of Plasma Sprayed Al_2O_3 + 13 wt% TiO_2 Coatings on a Low Carbon Steel, *Surf. Coat. Technol.,* Vol 52, 1992, p 141-144
92. W. Aihua, Z. Beidi, T. Zengyi, M. Xianyao, D. Shijun, and C. Xudong, Thermal-Shock Behavior of Plasma Sprayed Al_2O_3 + 13 wt% TiO_2 Coatings on Al-Si Alloy Influenced by Laser Remelting, *Surf. Coat. Technol.,* Vol 37, 1993, p 169-172
93. I. Zaplatynski, Performance of Laser-Glazed Zirconia Thermal Barrier Coatings in Cyclic Oxidation and Corrosion Burner Rig Tests, *Thin Solid Films,* Vol 95, 1982, p 275-284
94. F.S. Galasso and R. Veltri, Observation of Laser Interaction with Ceramics, *Am. Ceram. Soc. Bull.,* Vol 62 (No 2), 1983, p 253-254
95. K.M. Jasim, D.R.F. West, W.M. Steen, and R.D. Rawlings, Laser Surface Sealing of Plasma Sprayed Yttria Stabilized Zirconia Ceramics, , *Laser Materials Processing, ICALEO'88,* G. Buck, Ed., Springer Verlag, 1989, p 17-30
96. K.M. Jasim, R.D. Rawlings, and D.R.F. West, Pulsed Laser Processing Of Thermal Barrier Coatings, *J. Mater. Sci.,* Vol 26, 1991, p 909-916
97. K.M. Jasim, R.D. Rawlings, D.R.F. West, Characterization of Plasma-Sprayed Layers of Fully Yttria-Stabilized Zirconia by Laser Sealing, *Surf. Coat. Technol.,* Vol 53, 1992, p 75-86
98. H.L. Tsai and P.C. Tsai, Performance of Laser-Glazed Plasma-Sprayed (ZrO_2-12 wt% Y_2O_3)/(Ni-22 wt% Cr-10 wt% Al-1 wt% Y) Thermal Barrier Coatings in Cyclic Oxidation Tests, *Surf. Coat. Technol.,* Vol 71, 1995, p 53-59
99. C. Chen, W.-C. Wei, and K.-J. Chang, Laser Remelting Process for Plasma-Sprayed Zirconia Coatings, U.S. Patent 5,576,069, 19 Nov 1996
100. Y. Fu, A.W. Batchelor, H. Xing, and Y. Gu, Wear Behavior of Laser-Treated Plasma-Sprayed ZrO_2 Coatings, *Wear,* Vol 210, 1997, p 157-164
101. A. Maricocchi, A. Bartz, and D. Wortman, PVD TBC Experience on GE Aircraft Engines, J. Therm. Spray Technol., Vol 9 (No. 2), 1997, p 193-199
102. T. Cosack, L. Pawlowski, S. Schneiderbanger, and S. Sturlese, "Thermal Barrier on Turbine Blades by Plasma Spraying with Improved Cooling," Paper 92-GT-319, presented at 37th ASME International Gas Turbine & Aeroengine Congress and Exposition, 1-4 June 1992
103. L. Pawlowski, Technology of Thermally Sprayed Anilox Rolls: State of Art, Problems, and Perspectives, *J. Therm. Spray Technol.,* Vol 5 (No. 3), 1996, p 317-335
104. J. Beczkowiak, H. Keller, and G. Schwier, Al_2O_3-TiO_2 Schichten-eine Alternative zu Cr_2O_3, *Thermische Spritzkonferenz TS96,* E. Lugscheider, Ed., Vol 175, DVS-Verlag, Düsseldorf, Germany, 1996, p 68-71
105. M. Groc, L. Pawlowski, I. Smurov, G. Clinton, and R. Pitt, Modeling of the Laser Engraving at Plasma Sprayed Cr_2O_3 Coatings on Anilox Rolls, *Thermal Spray: Practical Solutions for Engineering Problems,* C.C. Berndt, Ed., ASM International, 1996, p 603-613
106. M. Groc, L. Pawlowski, and I. Smurov, Modeling of the Laser Engraving at Plasma Sprayed Al_2O_3, TiO_2, and Al_2TiO_5 Coatings for Anilox Rolls, *Thermal Spray: A United Forum for Scientific and Technological Advances,* C.C. Berndt, Ed., ASM International, 1997, p 41-49
107. *Catalog of Zed Instruments,* Hersham, Surrey KT12 3PD, England, 1993
108. E. Meiners, Mikrostrukturierung von Makrooberflächen-Laseranwendungen in der Druckformenherstellung, *6th European Conference on Laser Treatment of Materials, ECLAT'96,* Vol 1, F. Dausinger, H.W. Bergmann, and J. Sigel, Ed., AWT, Stuttgart, Germany, 1996, p 663-674
109. E. Birch, Applied Laser Engineering Ltd, West Molesey, Surrey, KT8 2QZ, England, private information, 1997

Peer Reviewed